Title
THE COSMIC-RAY NEUTRON ENERGY SPECTRUM

Authors
Hess, Wilmot N.
Patterson, H. Wade
Wallace, Roger
et al.

Publication Date
1959-02-06

UCRL-8628

UNIVERSITY OF CALIFORNIA

Radiation Laboratory

BERKELEY, CALIFORNIA

UCRL-8628

UNIVERSITY OF CALIFORNIA
Lawrence Radiation Laboratory
Berkeley, California

Contract No. W-7405-eng-48

THE COSMIC-RAY NEUTRON ENERGY SPECTRUM

Wilmot N. Hess, H. Wade Patterson, Roger Wallace, and Edward L. Chupp

February 6, 1959

Printed for the U. S. Atomic Energy Commission

THE COSMIC-RAY NEUTRON ENERGY SPECTRUM

Wilmot N. Hess, H. Wade Patterson, Roger Wallace, and Edward L. Chupp

Lawrence Radiation Laboratory
University of California
Berkeley, California

February 6, 1959

ABSTRACT

The cosmic-ray neutron energy spectrum in the equilibrium region of the atmosphere has been measured with several different calibrated detectors from thermal energies to about 1 Bev at 44^{o} north magnetic latitude and up to 40,000 feet. By combination of the data from these measurements with those from other experiments, a complete differential energy spectrum is obtained which shows the characteristic maximum near thermal energies and a roughly 1/E variation up to about 100 kev. The presence of a second maximum in the spectrum near 1 Mev is attributed to the evaporation neutrons from stars, and above this energy up to 800 Mev the spectrum falls off as $E^{-1.4}$.

THE COSMIC-RAY NEUTRON ENERGY SPECTRUM*

Wilmot N. Hess, H. Wade Patterson, Roger Wallace, and Edward L. Chupp†

Lawrence Radiation Laboratory
University of California
Berkeley, California

February 6, 1959

INTRODUCTION

The cosmic-ray neutrons found in the earth's atmosphere are essentially all generated by interactions of the primary and secondary cosmic rays with the nitrogen and oxygen of the air. The primary cosmic rays[1] are made up of about 85% protons, 13% alpha particles, and 2% particles of $Z \geqslant 2$, and there is no evidence at this time indicating any appreciable flux of neutrons in the primary radiation. Because of the short neutron half life (~12 min) it is unlikely that a significant number of neutrons could reach the earth from regions more distant than the sun.

The neutrons in the range 10 Mev to 1 Bev are generated by direct processes such as penetrating showers, nuclear stars, or charge-exchange events, while in the 1-Mev region most neutrons come from the nuclear evaporation process. The neutrons in this region of the spectrum are moderated by inelastic and elastic collisions with nitrogen and oxygen nuclei and are eventually captured by the $N^{14}(n,p)C^{14}$ reaction or by other inelastic events. A few of the neutrons escape from the top of the atmosphere and eventually decay to protons. These albedo neutrons contribute to the cosmic radiation belt[2] observed by U. S. and U.S.S.R. satellites.

A study of the broad cosmic-ray neutron energy spectrum might shed light on related geophysical or geochemical problems, such as the C^{14} dating

* Work done under the auspices of the U. S. Atomic Energy Commission.

† Present address, Pilotless Aircraft Division, Boeing Airplane Company, Seattle, Washington.

process. Also an accurate determination of the spectrum could serve to verify the predictions of nuclear cascade theories for the atmosphere.

The present experiment was carried out over a period of two and a half years, beginning in the summer of 1956 at the 10,000-foot White Mountain Laboratory of the University of California near Bishop, California. During the winter of 1956-57 measurements were made at various altitudes up to 40,000 feet on nine flights in a B-36 bomber operating out of Kirtland Air Force Base in Albuquerque, New Mexico; and during the last year the detectors have been operated at sea level at the Engineering Field Station of the University of California and have been calibrated at the Lawrence Radiation Laboratory by use of a variety of standard neutron sources and the 184-inch synchrocyclotron in Berkeley. Also in the summer of 1958 a gold foil detector was exposed at the summit laboratory on White Mountain at 14,000 feet and later calibrated with the water-boiler reactor (WBNS) at the Lawrence Radiation Laboratory in Livermore, California.

DETECTORS

During the past ten years the Health Physics Group at the Lawrence Radiation Laboratory, under the direction of Professor Burton J. Moyer, has developed a series of instruments for measuring neutron fluxes in different energy regions. These instruments have been used primarily to measure stray radiation fields near accelerators, and could be adapted for study of cosmic-ray-produced neutrons. The neutron detectors that were used in this experiment are discussed below.

Bismuth-Fission Ionization Chambers

The Bi^{209} nucleus undergoes fission if struck by neutrons or protons of energy $E > 50$ Mev. Accordingly a high-threshold nucleon counter can be built in which the fission fragments are counted in an ionization chamber. A chamber has been built which has 63 g of Bi deposited in layers of 1 mg/cm^2 thickness on parallel Al plates. These plates are connected to one another in such a way that they act as the capacitors in a lumped-constant transmission line and minimize the over-all capacity as seen by any one plate.[3] The chamber is filled with 95% argon and 5% CO_2. In order to distinguish between events originating in the Bi itself and events originating in other chamber materials, an identical counter was made with no Bi on the plates; the difference between the counting rates of the two chambers is the effect of the Bi alone. This counter is also sensitive to mesons. The measured response to γ rays is small. A blanket of G-M tubes around the chamber permits the charged-particle-induced fissions to be separated from the neutral-particle-induced fissions, while the γ-ray component can be separated by running a Pb absorption curve. Shower events can be eliminated by study of the shapes of the photographically recorded chamber pulses. The π-meson cosmic-ray flux is small enough to be neglected. The μ-meson flux is not small, but the cross section for μ-induced fission of Bi is very small, so that, this reaction can be neglected. In this way the effect of the neutrons alone can be determined. The response of the chambers to the large Bi^{209} fission pulses (~80 Mev per fission) was insured by calibrating the chamber pulse height with a Cf^{252} spontaneous fission source (~100 Mev per fission).

CH_2-Lined Proportional Counter

An argon-and-CO_2 proportional counter has also been developed in which the recoil protons from neutrons hitting a polyethylene lining in the counter are counted.[4] For a 1/8-inch-thick polyethylene lining the efficiency of the chamber is nearly proportional to energy for neutrons from about 50 kev to about 20 Mev. Because of this, this counter actually records energy flux instead of the usual particle flux, and for this counter one count at zero bias corresponds to about 15 Mev/cm^2 of neutrons through the chamber. The efficiency of this chamber has been calculated and checked by placing the counter in neutron beams of known energies and fluxes. This chamber also counts protons and electrons, but the electron pulses are generally small enough to be separated out by pulse-height rejection. The effect of protons was accounted for by placing this counter under the blanket of G-M tubes used for the Bi chamber.

BF_3 Counter and Paraffin Jackets

A BF_3 proportional counter counts neutrons by the reaction $B^{10}(n, \alpha)Li^7$, and gives a uniform pulse height for neutrons in the thermal energy region. Since the cross section is proportional to 1/v, the counter responds primarily to thermal neutrons. If a cadmium cover is used, the thermal neutrons are absorbed and only the neutrons of $E \gtrsim 0.4$ volt are counted; however, if paraffin is placed around the chamber and a cadmium cover placed outside this, then the energy dependence is changed, since the paraffin thermalizes higher-energy neutrons and makes more of them count in the BF_3 counter. This counter has the advantage that it can be set to accept only the large ionization pulses (~4 Mev) from the alpha particle and Li^7, and to not count protons or γ rays.

Gold-Foil Resonance Detector

The cross section for gold has a resonance at 4.9 ev for capturing neutrons, and the product nucleus Au^{198} decays with a half life of 2.7 days by emitting a β particle which is followed by emission of a strong (99%) 412-kev gamma ray from the first excited level of Hg^{198}. Since this gamma ray can be easily detected by a NaI pulse-height-analyzer spectrometer, a neutron detector can be constructed that is essentially sensitive only to resonance neutrons.

An array of 0.0005-in. gold foils covering a 20 X 20-in. area was used as the detector. The top and bottom of this array were covered with cadmium to prevent thermal neutrons from being captured by the gold. A 3-in. layer of CH_2 was placed under the detector to minimize albedo effects from neutrons of energy up to several Mev reflected from the earth. The gold foils were exposed to cosmic-ray neutrons at an altitude of 14,000 feet for 10 days, removed from the assembly, stacked on top of one another, and counted by a NaI scintillation spectrometer 3 in. in diameter and 3 in. long.

Simpson Pile

A Simpson pile[5] was made to monitor the intensity of the star-forming radiation. This consisted of a pair of BF_3 counters mounted inside the flanges of a lead "I" beam covered by several inches of paraffin. The data from this instrument were not used in deducing the cosmic-ray neutron energy spectrum, since the efficiency and energy response of the device are not accurately known; it was used primarily as a relative monitor to compare different sets of measurements and to insure that there had been no time variations of the primary radiation. Simpson has shown that the neutrons in the equilibrium region of the atmosphere are produced primarily by the lower-energy primary radiation,[6] and because of their low momenta these primaries are more subject to perturbations of any magnetic and electric fields in space. Since the neutron measurements described here were carried out at several different latitudes and altitudes, this monitoring was important.

COLLECTION OF DATA

In the summer of 1956 all the detectors were taken to an elevation of 10,500 feet at the Crooked Creek Laboratory on White Mountain operated by the University of California; Professor Nello Pace, Director. The equipment was mounted in a trailer and power was supplied by a motor generator set. The equipment ran 24 hours a day for 2 months with no serious troubles. The counting rates of all the detectors were measured accurately and checks made of reliability and consistency. A block diagram of the electronics used is shown in Fig. 1.

The data from the Bi fission counter were recorded photographically from an oscilloscope trace as well as by a scaler. The counting rate was low enough that real pulses had to be visually identified so as to eliminate noise pulses(such as motor sparking). The data from the G-M counters were also presented on the film so that one could tell whether a charged or a neutral particle had induced the fission event and from what direction the particles had come. Data from the other counters were taken by scalers.

Each day the following checks were made on the apparatus:

1. A pulse-height spectrum of the Cf^{252} spontaneous fission source was taken on film and on the scaler. This checked the over-all gain and operation of the Bi fission system. The gain of the linear amplifier was changed to keep the total gain constant. Changes of more than 1 db were infrequent.
2. The oscilloscope was calibrated with a stable pulse generator.
3. The discrimination levels of the discriminators and scalers recording the Bi fission data were checked.
4. The counting rate of the CH_2 -lined proportional counter was checked with a Ra-Be neutron source. This checks the gain of the system, since the counting rate is a quite sensitive function of the gain.
5. The counting rate of each group of G-M tubes covering the Bi fission counter was determined, and individual tubes were checked to see that they appeared to count normally.
6. The Simpson pile counting rate for a Ra-Be neutron source was measured. No changes of more than 1% were ever seen for the Simpson pile, either in calibration or in day-to-day use other than those correlated with barometric pressure changes.

7. The BF_3 counter with CH_2 covers of different thicknesses was calibrated daily with the Ra-Be neutron source.

Small changes in counting rate were observed at White Mountain in several detectors which were correlated with pressure changes. The changes were not corrected for, since they were small and tended to average out with time.

During the Fall of 1956 the equipment used at White Mountain was taken to Kirtland Air Force Base in Albuquerque, New Mexico, and installed in the aft compartment of a B-36 bomber. Certain precautions were taken to avoid spurious counts arising in the plane: (a) All the electronics equipment and all the counters (except the Simpson pile) were shock-mounted to minimize vibration problems, and (b) various power fittings were changed to prevent arcing at low pressures. During flight, 400-cycle current was used (with no modification to the 60-cycle equipment). We found that when we were changing altitude rapidly, we encountered problems with noise in the electronics which may be due to variation in the earth's electric field with altitude. During level flight noise problems were rarely noticed and all equipment functioned properly. Calibrations of all counters were made in flight and found to agree with data taken on the ground. Figure 2 shows routes of the different flights.

Several checks were made to see that the counting rates of our detectors were not functions of the local environment. For example, the counting rate of a bare BF_3 counter might depend on the amount of gasoline in the tanks of the plane. We looked for and found no significant effects of this kind.

CALIBRATION OF THE COUNTERS

In order to determine the energy spectrum of the cosmic-ray neutrons one must know the absolute energy sensitivities of the several counters and in order to measure these, we placed the counters in various neutron beams of known energy and flux and measured the counting rates. The different neutron sources used with the counters, and their characteristics, are summarized in Table I. The results of this calibration procedure for the polyethylene-lined proportional counter is shown in Fig. 3 (Curve A), which indicates the efficiency of the counter increasing linearly with energy from 300 kev to about 15 Mev. This curve demonstrates that the proportional

Table I. Neutron sources

Type of Source	Average Neutron Energy	Counter calibrated
Sb - γ - Be	25 kev	BF_3 + various thicknesses of paraffin, Proportional counter
Po - α - Li	400 kev [a]	BF_3 + various thicknesses of paraffin, Proportional counter
Mock fission	1.4 Mev [a]	BF_3 + various thicknesses of paraffin, Proportional counter
Po - α - Be	4.4 Mev [a]	BF_3 + various thicknesses of paraffin, Proportional counter
D - T	14.5 Mev (Monoenergetic)	BF_3 + various thicknesses of paraffin, Proportional counter
184-inch cyclotron neutron beam	220 Mev	Bi fission counter

[a] For neutron energy spectra of α, n sources see Hess.[8]

counter is in effect an energy-flux counter, and not a particle-flux counter.

The efficiency of the bare BF_3 counter was calculated from the known thermal B^{10} $(n, \alpha)Li^7$ cross section and the volume and pressure of the counter. Following the notation of Yuan,[7] we calculated the effective area of the bare counter that we used as 2.6 cm^2 for thermal neutrons. By calculating the efficiency of the counter used by Yuan one obtains an effective area of 5.1 cm^2 compared with 5.1 ± .6 cm^2 obtained by Yuan when calibrating his counter in a reactor thermal-neutron beam. The calculation is probably more accurate than the calibration experiment.

The efficiency of the BF_3 counter with a cadmium cover can be obtained from the efficiency of the bare counter and the known cross section for cadmium. From the efficiency curves for the BF_3 counter with various thicknesses of paraffin covers (shown in Fig. 4) obtained by using a Po-Be neutron source for different angles θ of the counter axis with respect to the source, one obtains the energy sensitivities, averaged over θ to represent an isotropic neutron flux, shown in Fig. 3 for different thicknesses of paraffin.

The Bi fission chamber has been calibrated in the neutron beam from the 184-inch cyclotron. The Bi fission chamber was placed in the neutral-particle beam of the 6.2-Bev Bevatron and the attenuation mean free path in concrete and lead was found, within the accuracy of the measurement, to be the same as that for cosmic-ray neutrons in air. The cross section for Bi fission is known quite well up to 340 Mev.[9] Only the cross section would be needed to indicate the energy sensitivity if all the bismuth were effective in making counts in the chamber, but the bismuth layer is nominally 1 mg/cm^2 thick, which is an appreciable fraction of a fission-fragment range. Therefore the counter must be calibrated in a known flux to determine the fraction of the bismuth that is effective. The efficiency of different thicknesses of Bi has recently been studied,[10] and it has been found that the Bi in this counter should be 90% efficient. The efficiency calculated from this and from the known Bi fission cross section and the known volume of Bi in the counter is shown in Fig. 5. The experimental point obtained at 200 Mev is also shown and the agreement is seen to be good. The no-bismuth counter was also exposed to the cyclotron neutron beam and it showed no large counts; however, there were some smaller counts which could be explained by spallation. All the events having reasonably large pulse heights are therefore assumed to be from Bi fission. Typical pulse-height spectra for the no-Bi and Bi-coated chambers when exposed to the cosmic-ray flux are shown in Fig. 6. Also shown is a normalized pulse-height spectrum from a thin Cf^{252} spontaneous-fission source used for checking the over-all performance of the system.

The gold foil detector was calibrated at the water boiler reactor at the Livermore Laboratory. This detector was activated in a beam that was at the same time calibrated by using other thin, calibrated, Cd-covered gold foils, which were later counted. From the activity of the calibration foils the value of k in the expression $\phi(E) = \frac{k}{E}$ was obtained. From the activity of the detector gold foils we get the efficiency, defined as the number of Au^{198} decays per unit of neutron flux incident on the detector. The estimated relative error in the value of k from this calibration is ~30% and is due almost entirely to the uncertainty in the extrapolated value of the cadmium ratio for a foil of zero thickness.

DETERMINATION OF THE COSMIC-RAY NEUTRON ENERGY SPECTRUM FROM THE EXPERIMENTAL DATA

The neutron energy spectrum calculated from the data presented here is shown in Fig. 7. It is convenient to consider the spectrum as made up of three energy regions:

Region 1--from thermal energies to 50 kev,
Region 2--from 50 kev to 1 Mev,
Region 3--from 1 Mev up.

The experimental data that aid in calculating the spectrum in Region 1 consist of:

(a) The C^{14}-production rate in the atmosphere.[11]

(b) The counting rate of a bare BF_3 counter, with and without a cadmium cover, measured by Yuan,[7] by Simpson,[5] and in this experiment.

(c) The counting rate of cadmium-covered gold foils exposed to cosmic rays, which gives the flux at 4.9 ev.

Other resonance detectors could be used to establish more clearly the low-energy end of the spectrum, but one difficulty with these measurements is that they should be carried out some distance above the earth so that the neutron-energy spectrum would not be influenced by the presence of materials other than oxygen and nitrogen.

The Shape of the Spectrum in Region 1

The spectral shape in the low-energy region is determined from two considerations; first, from 10 kev down to about 1 ev, the spectrum has roughly a 1/E energy dependence. This is a straightforward result of neutron slowing-down theory, and applies for any mixture of moderating materials provided that the energy region under consideration is sufficiently below the energy at which the neutrons are produced and also that there is no absorption taking place.[12] For an infinite nonabsorbing medium if the scattering cross section is independent of energy the spectrum goes exactly as 1/E, but when fast-neutron leakage or absorption occurs or if there is an energy-dependent cross section then the spectrum is modified and the spectrum energy dependence is given approximately by $1/E^{\alpha}$. An estimate of the effect of leakage of neutrons out of the atmosphere shows that it will not contribute to make α deviate from 1 except quite near the top of the atmosphere. Calculations of absorption show that the (n,γ) process contributes slightly even at 50 kev, but the energy dependence of the cross section is the major factor in making $\phi(E) \propto 1/E^{0.88}$. This is the energy dependence shown from 1 ev to 50 kev in Fig. 7. Above 50kev one approaches the energy at which evaporation neutrons are produced (~1 Mev) and therefore the 1/E spectrum is modified by the source spectrum. In the 1-ev region, neutron absorption by nitrogen is an important process, and the shape of the energy spectrum depends upon the details of the absorption process, which competes with thermalization of the neutrons. This problem was first considered by Bethe, Korff, and Placzek,[13] who worked out the resonance-escape probability for a 1/v absorption by nitrogen and obtained the low-energy spectrum shown in Fig. 8 (Curve B). Modifications of this same treatment have been made by Fermi[14] (Curve C on Fig. 8) and also by Freese and Meyer[15] (Curve D on Fig. 8). This same subject is discussed by Pool, Nelkin, and Stone,[16] who give a more exact treatment. Their results are shown as Curve A in Fig. 8. Davis has also worked on this problem.[17] As one can see by inspection of Fig. 8, the various theoretical analyses do not differ radically, and it is hard to distinguish between them experimentally. One possible method of differentiating them would require accurate measurements of the cadmium ratio, that is, the counting rate of a BF_3 counter without the cadmium counter divided by the counting rate of a BF_3 counter with a cadmium cover. Unfortunately this is not very sensitive to the rather small difference in the spectrum shown in Fig. 8; for example, all the spectra shown give cadmium ratios of about 2.2:1. Another way of distinguishing the spectra would involve activation of different material having resonances in regions where the spectra are different. Because the treatment by Pool, Nelkin, and Stone seems to be the most exact, it was used for the low-energy spectral shape, thus permitting the determination of the absolute differential energy spectrum N(E), in Region 1 from the counting rates of the different detectors. The counting rate of a detector is given by

$$C_i = \int N(E)\, \Sigma_i(E)\, dE,$$

where C_i = counts/sec, N(E) = neutrons/cm^2-sec-Mev, $\Sigma_i(E)$ = counts/neutrons/cm^2. Knowing the detector efficiency, $\Sigma(E)$, absolutely, and the shape of the differential energy spectrum, one can obtain the absolute value of N(E) by doing a series of numerical integrations to get a value C_i in agreement with the data. The largest uncertainty in the spectrum obtained in this manner is the choice of a particular spectrum shape.

Region 2--from 10 kev to 1 Mev

The detector that gives useful information in this energy interval is a BF_3 counter used with several different thicknesses of paraffin coverings. As more paraffin is added around the BF_3 counter, higher-energy neutrons are detected. The counting rates for a series of paraffin covers on a BF_3 counter were measured at White Mountain and at airplane altitudes, and a family of these paraffin build-up curves is shown in Fig. 9. The spectrum in the region from 10 kev to 1 Mev is calculated from these counting rates by use of the equation above. The energy dependence of the spectrum is not known in this region, but the average height of the spectrum in the energy region of the BF_3 counter with one particular thickness of CH_2 jacket can be calculated from the integral. Then by comparison of the results of this process for the counter with different thicknesses of CH_2 the spectrum energy dependence is obtained roughly. An iteration process yields the spectrum accurately. It turns out that the 1/E spectral shape cannot be used in this energy region because it would give too high counting rates for the thick CH_2 covers. The shape of this portion of the spectrum shown in Fig. 7 is fairly unique. An experiment has been performed by Gross using 190-Mev protons incident on carbon nuclei and the resulting evaporation-neutron spectrum has been measured.[18] Since this experiment should give results quite comparable to those obtained from high-energy cosmic-ray nucleons incident on nitrogen or oxygen nuclei, the shape of this spectrum has been used to obtain the shape of the peak at 500 kev shown in Fig. 7. The height of the spectrum at 50 kev was determined not only from the data from the BF_3 counter plus paraffin covers, but also from the fact that the spectral height below 50 kev had already been determined (as discussed earlier under Region 1). The height at 50 kev from the analysis of the data for BF_3 plus paraffin in Region 2 was made to agree with these lower-energy data.

We believe that the spectrum shown in Fig. 7 is accurate to about ± 25% at all energies, with the exception of the region below .04 ev. Differences of a factor of 2 or more in the very low energy end of the spectrum are seen in the different theoretical spectra shown in Fig. 8 and there is no experimental information on which to base a selection of any one of these.

Region 3--from 1 Mev Up

The experimental data that enable one to calculate the spectrum in this region consist of:

(a) The abundance of cosmic-ray neutron-induced stars in photographic emulsions.

(b) The counting rate of the large bismuth fission ionization chamber.

(c) The counting rate of the polyethylene-lined proportional counter.

The energy intervals in which these detectors are important are shown in Fig. 10. Actually what is plotted in Fig. 10 is the product of the efficiency $\Sigma(E)$ of the detector times the height of the neutron spectrum N(E). The integrals under these curves gives the counting rates for these detectors. (The curves were terminated at the low-energy end when 98% of the counting rate had been included under the curve.) By inspection of the curves one can see that the nuclear emulsions and the bismuth fission chamber give information about neutrons with the energy interval roughly 100 to 500 Mev. The polyethylene-lined proportional counter gives information from about 100 kev to about 10 Mev. The shape of the spectrum in Region 3 is calculated by taking the counting rates of these detectors and--by the same trial-and-error procedure as described for Region 2--finding that shape of the curve which gives all the counting rates to within 10%.

The shape of the composite spectrum shown in Fig. 7 appears quite reasonable and as a comparison an approximate spectrum from a nuclear reactor[19] is shown in Fig. 11, which shows a peak at about 1 Mev due to the production of neutrons by the fission process. From about 10 kev down to about 1 ev the spectrum in Fig. 11 has a 1/E shape. The peak below 1 ev is the thermal neutron group. In the atmosphere cosmic-ray neutrons cannot show the thermal group seen in Fig. 11 because nitrogen is a better slow-neutron absorber than reactor materials. Also in cosmic rays there are present a considerable number of neutrons of energies higher than from the fission spectrum. Aside from these points the cosmic-ray spectrum shown in Fig. 7 is quite similar to the reactor spectrum in Fig. 11.

The spectrum shown in Fig. 7 is for 200, 700, and 1030 g/cm^2 atmospheric depth and for a geomagnetic latitue[20] of 44^o north. Data taken at other latitudes was converted to 44^o by using the neutron latitude variation measured by Simpson.[5] Our measurements indicate that the shape of the spectrum is unchanged from 200 g/cm^2 to 1030 g/cm^2 (sea level). Figures 12a and 12b show the attenuation curves for the Bi fission chamber and for the BF_3 counter with no $(CH_2)n$ but with a Cd cover. The fact that the attenuation mean free paths for these two counters are experimentally equal indicates that the spectrum from about 1 ev to about 500 Mev does not change shape from 200 g/cm^2 to 1,000 g/cm^2 depth in the atmosphere. Above 200 g/cm^2 the spectrum will probably be found to change shape. Near the top of the atmosphere there should be fewer low-energy neutrons, since the thermalization process will not be in equilibrium. The albedo from the lower atmosphere, where equilibrium has been established, will tend to make this effect small, but it will probably be present. Near the surface of the earth albedo effects from the ground or water may modify the spectrum. Both earth and water should absorb fewer neutrons than air so that the spectrum near the bottom of the atmosphere might be rich in thermal neutrons reflected upwards. Work by Mather indicates that the earth tends to thermalize incident neutrons without capturing many of them, and then the slow neutrons are mostly reflected into the air and eventually captured by N^{14}.[21]

If one assumes a power-law spectrum for the primary cosmic-ray protons then according to Messel's theory of the nucleon cascade the differential spectrum of those secondary nucleons above the primary cut-off energy E_c should have the same shape as the primary spectrum.[22] On the basis of this argument the spectra shown in Fig. 7 may be extended above 3 Bev (E_c at 44°) by using the power law given by Singer for the primary spectrum which has an exponent of 2.15 for the differential form for proton.

Table II is a summary of the counting rates of the various detectors used and the counting rates of these detectors calculated from the measured efficiencies and from the height of the neutron energy spectrum shown in Fig. 7. After we had concluded this experiment we became aware of the work of Miyake, Hinotani, and Nunogaki on the cosmic-ray neutron-energy spectrum.[23] They measured the spectrum in the energy region 1 to 15 Mev. They studied proton recoils in a cloud chamber and calculated the spectrum fron 1 ev to 1 Bev by considering the slowing down of neutrons and subsequent capture on nitrogen and also the production of high-energy neutrons. Their spectrum is shown in Fig. 7 integrated over solid angle and translated in latitude to compare to ours. There is reasonably good agreement between their spectrum and the spectrum calculated here. In the ev energy region the agreement is good and above 10 Mev it is very good. For intermediate energies our spectrum is probably more reliable because (a) we had experimental information in the region 100 kev to 1 Mev, and (b) we included neutron absorption in the spectrum calculations.

Table II

Experimental counting rates vs. counting rates calculated from our spectrum (All data for 700 g/cm^2 and 44^o geomagnetic latitude)

Detector	Calculated from Spectrum	Experimental
Au Foil (K value)	4.9×10^{-3} neutrons/cm^2-sec	$5.0 \pm 1.7 \times 10^{-3}$ neutrons/cm^2-sec
BF_3 + 1/2" CH_2	.097 counts/sec	0.084 counts/sec ± .005
BF_3 + 1" CH_2	.141	0.150 ± .006
BF_3 + 1-1/4" CH_2	.168	0.173 ± .006
BF_3 + 1-1/2" CH_2	.212	0.192 ± .006
BF_3 + 2" CH_2	.250	0.208 ± .005
BF_3 + 3" CH_2	.221	0.200 ± .008
BF_3 + 4" CH_2	.136	0.133 ± .006
BF_3 + 5" CH_2	.098	0.105 ± .006
Proportional counter	1.46 counts/min	1.55 ± .18 counts/min
Bi fission	1.33 counts/hr	1.6 counts/hr ± .3
Stars in emulsions	15 stars/cm^3-day	15 stars/cm^3-day [a]
C^{14} atoms produced/cm^2-sec	3.1 atoms/cm^2-sec	2.6 atoms/cm^2-sec [b]
BF_3 + no paraffin + Cd cover	.0022 counts/cm^2	0.0026 ± .0003 counts/cm^2 [c,d]

[a] See Lock et al.[26]

[b] Anderson and Libby.[11]

[c] Yuan.[7]

[d] For a counter of 1 cm^2 thermal effective area.

THE NUCLEON CASCADE

Rossi has made a simple model of the medium-energy nucleon cascade in the atmosphere[24] that is probably not too far from reality. The cascade is limited to one dimension, and the production spectrum of both neutrons and protons, based on the work of Camerini,[25] is taken to be

$$S(E, h) = \frac{Ae^{-h/L}}{(50+E)^2},$$

where h = depth into the atmosphere, L = attenuation mean free path, E = kinetic energy. This is not very different from the currently accepted primary proton spectrum shape. The differential-energy spectra of the secondary particles produced in the cascade are then for neutrons,

$$\phi_n(E, h) = \frac{Ahe^{-h/L}}{(50+E)^2},$$

and for protons,

$$\phi_p(E, h) = \frac{Ae^{-h/L}}{k(E)} \left[\frac{Em - E}{(50+E)(50+E_m)} \right],$$

where $k(E) = \frac{dE}{dh}$ = ionization energy-loss rate of protons and E_m is defined by $R(E_m) = R(E) + h$. If we integrate the area under this spectrum (for L = 138 g/cm^2) from high energies down to 80 Mev, we can get the ratio of secondary protons to neutrons of energies greater than 80 Mev as a function of atmospheric depth (Fig. 13). This can be compared with the fraction of events in the Bi fission chamber that are induced by charged or by neutral particles (i.e., have or have not a G-M signal in coincidence). Since Rossi's spectra are for secondary particles only, we must add the primary protons ϕ'_p to get the total number of protons, or $\phi_p + \phi'_p$. The ratio T of neutral to charged events (Fig. 13) that we find experimentally is then

$$T = \frac{\Phi_n}{\Phi_p + \Phi'_p} = \frac{\Phi_n/\Phi_p}{1 + \Phi'_p/\Phi_p} = \frac{R}{1 + U},$$

Where R is the ratio of secondary neutrons to secondary protons Φ_n/Φ_p that we calculate from Rossi's spectrum, and U is the ratio of primary protons to secondary protons, Φ_p/Φ_p. Using this relationship, the measured value of T, and the calculated value of R, one obtains the values of U shown in Fig.14 as a function of h, the depth into the atmosphere.

According to the treatment by Rossi, we can calculate an approximate value of $U = \Phi'_p/\Phi_p$ in the following way. Let us take for the differential spectrum of primary protons, at some depth h into the atmosphere,

$$\phi'_p(E, h) = \phi'_p(E)e^{-h/L},$$

where L contains the effect of slowing down the protons by ionization energy loss as well as loss by nuclear interactions. Then the secondary-proton differential spectrum is given by[24]

$$\phi_p(E, h) = \overline{C(h)} \iint m(E, E')\, N\sigma \phi'_p(E)e^{-h/L}\, dh\, dE',$$

where m(E, E') is the average number of secondary protons of energy E made by protons of Energy E', and C(h) is an approximate correction factor to take care of the energy loss by ionization of secondary protons produced above altitude h. The value of C must be averaged through the depth h above the position in question, because the secondaries have come from all positions above h. If now we ask how many primary and secondary protons of energy E >80 Mev we have at any depth h, we can use an average secondary multiplicity $\bar{m}$ (which can be obtained from emulsion data),[25] and then integrate the spectra from 80 Mev up; we obtain, for the primaries,

$$\Phi'_p\,(E>80, h) = \Theta\, e^{-h/L} = \int_{80}^{\infty} \phi'_p(E')e^{-h/L}\, dE',$$

and for the secondaries,

$$\Phi_p(E>80\,, h) = \overline{C(h)} N\sigma\, H\, \bar{m} \int_0^h e^{-h/L}\, dh$$

$$= \overline{C(h)}\, N\sigma\, H\, \bar{m}\, L_{eff} \left[e^{-h/L} - 1 \right].$$

Taking $C(h) = e^{-h/p}$, we then get

$$\overline{C(h)} = \frac{1}{h} \int_0^h C(h)\, dh = \frac{T}{h}\left[e^{h/p} - 1\right],$$

which gives

$$U = \frac{h}{\bar{m}\, N\, \sigma\, L_{eff}\left[e^{h/L} - 1\right]\; p\left[e^{h/p} - 1\right]}.$$

Using the inelastic cross section σ per "air" atom as 0.25 barn, and using $p = 1450\ g/cm^2$ (obtained from the Rossi secondary-proton spectra) and $L = 148\ g/cm^2$ (also obtained from the Rossi spectra) and $\bar{m} = 0.36$ from emulsion data, we get the solid curve shown on Fig. 14.

RESULTS AND CONCLUSIONS

We have determined the cosmic-ray neutron energy spectrum in the equilibrium region of the atmosphere. The principal features of the spectrum seem quite reasonable. Prior to this work most of the experimental studies of the neutron spectrum had concentrated in small regions of the spectrum, either the thermal region or the 100-Mev region (stars in emulsions). In this study we have attempted to cover as much of the spectrum as possible. One result of this wide energy survey has been the discovery of the evaporation peak in the spectrum at about 1 Mev. The conclusion that this peak is present because there is a strong source of evaporation neutrons is not too surprising. A nuclear reactor shows a peak in the spectrum at about the same energy as the energy of its neutron source--namely, fission neutrons.

The principal reason for measuring the cosmic-ray neutron-energy spectrum is to provide a basis for testing the theories on the nuclear cascade process in the atmosphere. However, a strict comparison of theory with experiment is not possible at this time because the main theory (Messel's) applies only to secondary nucleons of energy >500 Mev. This is near the effective upper limit of the Bi fission chamber (i.e., cross section unknown above). In the region from 10 to 500 Mev, the present spectrum shows the $E^{-1.5}$ fall-off--about the same behavior as the data of Camerini on stars in emulsions.

Since the shape of this cosmic-ray neutron spectrum should be comparable to that from shielded high-energy accelerators, it should be useful for determining the background spectra around such accelerators for physics experiments and also for determining the personnel hazard from neutrons. This spectrum has also recently been used for estimating the neutron dose expected for persons spending long periods of time in a high-altitude environment.[34]

For an accurate determination of the neutron-energy spectrum it is important to know if any short-period time variations could contribute to the difference in intensities observed with the various detectors at different latitudes and altitudes. No significant changes were observed in the Simpson pile counting rates that might be correlated with changes in the primary radiation.

It is well know that there are no diurnal variations for the neutrons counted with the BF_3 counter. It is concluded from the data taken at White Mountain with a Bi fission chamber that there is no diurnal variation greater than 10% for neutrons of energy greater than 80 Mev.

No attempt was made to determine if the 27-day cycle observed by Simpson exists also for higher-energy neutrons. This effect could be expected since these neutrons and those detected by a Simpson pile are probably produced by the same region of the primary spectrum, i.e., the low-energy primaries.

We conclude that the spectrum given in Fig. 7 represents the true spectrum in the equilibrium regions of the atmosphere unperturbed by time variations of the primaries.

An attempt is now being made to calculate the neutron spectrum by using an evaporation spectrum peaked at about 1 Mev as a source function. If this is successful it will enable us to calculate the cosmic-ray neutron albedo. The decay of these albedo neutrons produces electrons and protons, some of which are trapped by the earth's magnetic field to produce at least part of the radiation belt observed by satellites.

ACKNOWLEDGMENTS

The authors would like to thank Professor Burton J. Moyer for his support and encouragement and advice during all phases of the experiment.

We would like to acknowledge the substantial contributions made to this experiment by Paul Manis and Joseph Wentworth, members of the University of California High-Altitude Research Station staff under the direction of Professor Nello Pace.

The experiment could not have been performed without the assistance of Colonel Herschel D. Mahon, 4925th Group Commander, who made it possible for us to make the B-36 flights. We would like to thank all the officers and men of the 4925th Test Group (Atomic) at Kirtland Air Force Base who helped us in the project, and our special thanks for their contributions go to the following members of the 4925th:

Major Fain Poole, 4928th Squadron Commander
Major Robert Lundin, 4928th Operations Officer
Captain Russell Weaver, Jr., Project Officer
Master Sgt. Roy Bedwell, Crew Chief
First Sgt. Roger Caron, Asst. Crew Chief

In addition we wish to thank William Goldsworthy and Lloyd Stephens of this Laboratory for their valuable assistance in all parts of the experiment, but especially in instrumentation and data recording. One of us (E. L. C.) would like to express his appreciation to Dr. Herbert F. York, Dr. John S. Foster, Jr., and to Dr. Chester M. Van Atta for their support in his participation in this work. Finally our sincere appreciation is expressed to Dr. N. Fred Wikner, now at General Atomics, San Diego, for many stimulating discussions about the calculations of the cosmic-ray neutron spectrum.

This work was done under the auspices of the Atomic Energy Commission.

APPENDIX

I. Data from Other Experiments

Besides the data taken in the present experiment there are several other sources of information that can be used to help obtain the cosmic-ray neutron energy spectrum.

Several authors[27-30] have measured the number of stars/cc/day in nuclear emulsions caused by the cosmic-ray N-component at different altitudes.

Table III

Intensity of the star-producing radiation

Reference	Residual pressure (g/cm^2)	Stars per cm^3 per day
George	1030	1.47
Bernardini	680	14.2
Lattimore	670	16.4
Lord	660	22
"	105	1610
"	15	2390

This information can be used to obtain data about the cosmic-ray neutron spectrum in the energy range near 100 Mev. The various authors listed in Table III define "stars" as events having three or more prongs. They normally cannot identify the incident particle in such an event if it is charged. Therefore, we can say that their cosmic-ray stars are composed of three-prong stars induced by neutrons, and two-prong stars induced by protons (in which the incident proton looks like a third prong). We will neglect π-meson-induced stars in this analysis, since there should be very few of them—especially at low altitudes. We will consider protons and neutrons to have the same cross section for n-prong star production. We can write the relation

$$C(x) = \int \frac{N_p(E)}{\lambda_2(E)} \, dE + \int \frac{N_n(E)}{\lambda_3(E)} \, dE,$$

where C(x) is the observed counting rate in stars/cc/sec, N_p is the flux of protons in protons/cm^2/sec/Mev, and N_n is the flux of neutrons/cm^2/sec/Mev, λ_2 is the mean free path for the production of stars having two or more charged prongs, and λ_3 is the mean free path for the production of stars having three or more charged prongs. We can find values of λ_2 and λ_3 in the literature on nuclear physics. Work on this subject has been done by Germain, Bernardini, Lock, and Johnson.[26] A summary of the values of λ obtained from their work is given in Fig. 15.

The data of Germain give directly the values of λ_2 and λ_3. The other authors give prong distribution which can yield values of λ_2 and λ_3, using the geometrical mean free path for emulsion nuclei properly averaged over the constituent elements as 29 cm.[31] The values of λ depend on the energy of the incident particle, as is shown in the accompanying graph. The λ values do not depend upon X, the depth in the atmosphere, and we are assuming that they are the same for neutron- or proton-induced events. In order to determine values for the neutron energy spectrum, $N_n(E)$, we must eliminate $N_p(E)$ from the earlier equation. We do this by assuming $N_p(E) = kN_n(E)$, and then can evaluate k.

At altitudes of 700 g/cm^2 or below most particles are secondaries. Therefore, we use Rossi's spectra[24] to get values for k. At 190 g/cm^2, we have said, the number of primary protons is two times the number of secondary protons (See Fig. 14). The primary-particle energy spectrum has been assumed to be of Rossi's form,[11] given by

$$N_p'(E) = \frac{A}{(E+50)^2} .$$

We get k for 190 g/cm^2 now by using $k = \dfrac{N_p(E) + N_p'(E)}{N_n(E)}$. Using these values of k and the values of λ_2 and λ_3, we can evaluate Q in the equation

$$C_h = \int_0^\infty Q(E,h)\, N(E)\, dE,$$

where

$$Q(E,h) = \frac{k(E,h)}{\lambda_2(E)} + \frac{1}{\lambda_3(E)} .$$

Values of Q are plotted on Fig. 16. From this graph of Q we see that the data on stars in emulsion give data about the cosmic-ray neutron energy spectrum in roughly the same energy region as the bismuth fission chamber.

II. Production of C^{14} in the Atmosphere

Most cosmic-ray neutrons, after slowing down, are captured in N^{14} by the process $N^{14}(n, p)C^{14}$. The C^{14} made this way is incorporated into plants, animals, carbonates in sea water, etc., and β-decays slowly back to N^{14}. If one measures the total amount of C^{14} in the biosphere and assumes that the cosmic-ray intensity has been constant for 30,000 years or more, then one can calculate the total number of cosmic-ray neutrons needed to produce this equilibrium amount of C^{14} in the following way:

$$\frac{dNc}{dh} = \int \sigma_{np}(E)\phi(E, h)N_n dE\, dh,$$

where h = depth into the atmosphere, N_c = atoms of C^{14} produced per cm^2/sec, σ_{np} = absorption cross section of nitrogen for neutrons. Integrating, one has

$$N_c = N_N \int dh \int \frac{k}{\sqrt{E}} \left[n(E)G(h) \right] dE,$$

where $\phi(E, h)$ = neutron energy spectrum, N_N = atoms/g of nitrogen. We have said the absorption cross section varies as 1/velocity,

$$\sigma_{nN}(E) = \frac{k}{E}$$

and that the shape of the neutron energy spectrum is independent of altitude, so that we have

$$\phi(E, h) = n(E)G(h);$$

now, the integral is

$$Nc = N_N k \int G(h)dh \int \frac{n(E)}{E}\, dE.$$

The first integral, which integrates the intensity through the depth of the atmosphere, can be evaluated from the altitude-neutron-intensity curves obtained by Korff.[32] The second integral can be obtained from the spectrum shown in Fig. 7.

The total amount of C^{14} calculated this way agrees to within 10% with the total amount measured by Libby and Anderson.[11]

III. Slowing Down and Diffusion of Slow Neutrons

It is of interest to see how far a neutron travels from its point of production during slowing down (L_s = slowing-down length), and then how far it diffuses after being thermalized (L_d = diffusion length) before being captured. Also we can calculate how long it takes to slow down (t_s = slowing-down time) and how long it diffuses (t_d = diffusion time) before capture.

We will consider an evaporation neutron made at 1 Mev. We can evaluate these quantities from the known scattering and absorption cross sections.[33]

Altitude	L_s	L_d	t_s	t_d
40,000 feet	1500 meters	340 m	0.65 sec	0.25 sec
Sea level	330 m	75 m	0.15 sec	0.06 sec

It can be seen from the table that the neutrons don't move very far from the point of birth to where they are captured. Also the time lived is so short that very few decay before capture. For higher-energy neutrons the slowing-down length is greater but the other quantities are not changed much.

REFERENCES

1. S. F. Singer, in Progress in Elementary Particle and Cosmic Ray Physics, John G. Wilson and S. A. Wouthuysen, Eds. (North-Holland Publishing Co., Amsterdam, 1958), Vol. IV., p. 278.
2. Nicholas C. Christofilos (UCRL), private communication, 1958; S. N. Vernov, Fifth General Assembly of CSAGI, Moscow, July 30-August 9, 1958; P. B. Kellogg, Nuovo cimento (in press); S. F. Singer, Phys. Rev. Letters 1, 171, 181 (1958).
3. Hess, Patterson, and Wallace, Nucleonics, 15, 74 (1957).
4. Burton J. Moyer, Nucleonics 10 No. 4, No. 5 (1952); Boyd W. Thompson, Nucleonics 13 No. 3, 44 (1955).
5. J. A. Simpson, Phys.Rev. 83, 1175 (1951).
6. J. A. Simpson, Phys. Rev. 80, 934 (1951).
7. L. C. L. Yuan, Phys. Rev. 81, 175 (1951).
8. W. N. Hess, Neutrons from (α, n) Sources, Annals of Physics (to be published).
9. Jungerman and Steiner, Phys. Rev. 101, 807 (1956) .
10. Beaslee, Hess, and Wallace (private communication).
11. Anderson and Libby, Phys. Rev. 81, 64 (1951); E. C. Anderson, Ann. Rev. Nuclear Sci. 2, 63 (1953); Willard F. Libby, Radiocarbon Dating (University of Chicago Press, Chicago, 1952).
12. See, for example, Samuel C. Glasstone and Milton C. Edlund, Elements of Nuclear Reactor Theory (D. Van Nostrand Company, Inc., New York, 1952), p. 158.
13. Bethe, Korff, and Placzek, Phys. Rev. 57, 573 (1940).
14. Enrico Fermi, Nuclear Physics (University of Chicago Press, Chicago, 1950), p. 221.
15. Werner Heisenberg, Kosmische Strahlung (Springer Verlog, Berlin, 1953).
16. Pool, Nelkin and Stone, Progress in Nuclear Energy, Physics and Mathematics, (Pergamon Press, London, 1958), Vol. II, p. 91.
17. William O. Davis, Phys. Rev. 80, 150 (1950).
18. Edward Gross, The Absolute Yield of Low-Energy Neutrons from 190-Mev Proton Bombardment of Gold, Silver, Nickel, Aluminum, and Carbon (Thesis), UCRL-3330, Feb. 1956.

19. R. L. Murray, Nuclear Reactor Physics (Prentice-Hall, Inc., Englewood Cliffs, N. J., 1957) p.42.
20. The magnetic coordinates we used were based on earth-surface-field measurements, not on cosmic-ray-inferred fields, since doubt has recently been cast on the latter (P. Rothwell, Phil. Mag. 3, 961 (1958)). We used $\sin \lambda_{mag} = \cos \Lambda (\cos \phi - 69) \cos 78.5 + \sin 78.5$, as quoted in Simpson, Fenton, Katzman, and Rose, Phys. Rev. 102, 1648 (1956).
21. R. Mather (Naval Radiological Defense Laboratory), private communication.
22. H. Messel, Progress in Cosmic Ray Physics, Vol. II, (Interscience Publishers, Inc., N. Y., 1954), p. 1761.
23. Miyaki, Hinotani and Nunogaki, J. Phys. Soc. of Japan 12, 113 (1957).
24. Bruno B. Rossi, High-Energy Particles (Prentice-Hall, Inc. New York, 1954) p. 488.
25. Camerini, Fowler, Lock, and Muirhead, Phil. Mag. 41, 413 (1950).
26. L. Germain, Phys. Rev. 82, 596 (1951); Booth, Bernardini, and Lundenbaum, Phys. Rev. 85, 826 (1952); Lock, March and McKeague, Proc. Roy. Soc. A231, 368 (1955); William R. Johnson, Multiple Meson Production in Emulsions Exposed to the Bevatron Beam (Thesis), UCRL-2979, May 1955.
27. E. P. George and J. Evans, Proc. Phys. Soc. A63, 1248 (1950).
28. Bernardini, Cortini, and Manfredini, Phys. Rev. 79, 952 (1950).
29. S. Lattimore, Phil. Mag. 40, 394 (1949).
30. J. J. Lord, Phys. Rev. 80, 901 (1951).
31. Walter Barkas (Lawrence Radiation Laboratory), private communication.
32. Neuberg, Soberman, Swetnick, and Korff, Phys. Rev. 97, 1276, (1955).
33. Donald J. Hughes and John A. Harvey, Neutron Cross Sections, Brookhaven National Laboratory report BNL-325, July 1955.
34. Patterson, Hess, Moyer and Wallace, The Flux and Spectrum of Cosmic-Ray-Produced Neutrons as a Function of Altitude, J. Health Physics (to be published).

FIGURE CAPTIONS

Fig. 1. Block diagram of the electronics.

Fig. 2. B-36 flights for cosmic-ray studies.

Fig. 3. Efficiencies of two detectors versus energy. Curve A is for the CH_2-lined proportional counter. The other curves are for the BF_3 counter; the thickness of paraffin (inches) covering it is shown for each curve.

Fig. 4. Efficiency of a BF_3 counter with various thicknesses of paraffin covers for counting Po-Be neutrons as a function of the angle of the counter axis to the source.

Fig. 5. Efficiency of the Bi fission counter as a function of energy.

Fig. 6. Pulse-height spectra for the Bi and no-Bi chambers. Also shown is a normalized spectrum for the CF spontaneous-fission source.

Fig. 7. The cosmic-ray neutron energy spectrum.

Fig. 8. Cosmic-ray neutron energy spectrum at low energies. All the curves have been normalized at 100 ev.

Fig. 9. CH_2 build-up curves for the BF_3 counter as a function of altitude in thousands of feet and north magnetic latitude.

Fig. 10. $\Sigma(E) \times N(E)$ for $BF_3 + CH_2$, proportional counter, Bi fission and emulsion stars, showing the relative regions of energy sensitivity.

Fig. 11. An approximate neutron-energy spectrum for a nuclear reactor.

Fig. 12. Attenuation curves for the Bi fission chamber and the BF_3 counter at 0-inch CH_2 through the atmosphere.

Fig. 13. Ratio of neutrons to protons of $E > 80$ Mev as a function of depth in the atmosphere. The solid curve is calculated from Rossi for secondary particles only.

Fig. 14. Ratio of primary protons to secondary protons as a function of depth in the atmosphere.

Fig. 15. Values as a function of energy of the reciprocal of the mean free path in emulsion for making two and three-prong stars.

Fig. 16. Values of Q as a function of energy for several depths in the atmosphere. Curve A is at 200 gm/cm^2, B at 700 gm/cm^2 and C at 1000 gm/cm^2.

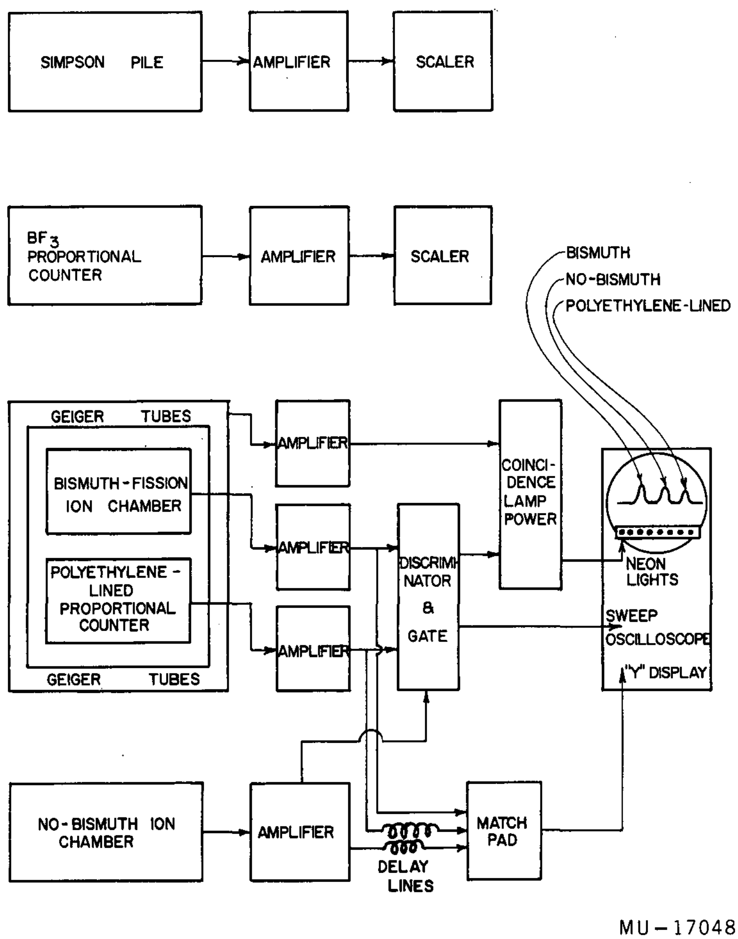
SIMPSON PILE
AMPLIFIER
SCALER
BF3 PROPORTIONAL COUNTER
AMPLIFIER
SCALER
BISMUTH
NO-BISMUTH
POLYETHYLENE-LINED
GEIGER TUBES
BISMUTH-FISSION ION CHAMBER
POLYETHYLENE-LINED PROPORTIONAL COUNTER
GEIGER TUBES
AMPLIFIER
AMPLIFIER
AMPLIFIER
DISCRIMINATOR & GATE
COINCIDENCE LAMP POWER
NEON LIGHTS
SWEEP OSCILLOSCOPE
"Y" DISPLAY
NO-BISMUTH ION CHAMBER
AMPLIFIER
DELAY LINES
MATCH PAD
MU-17048

Fig. 1.

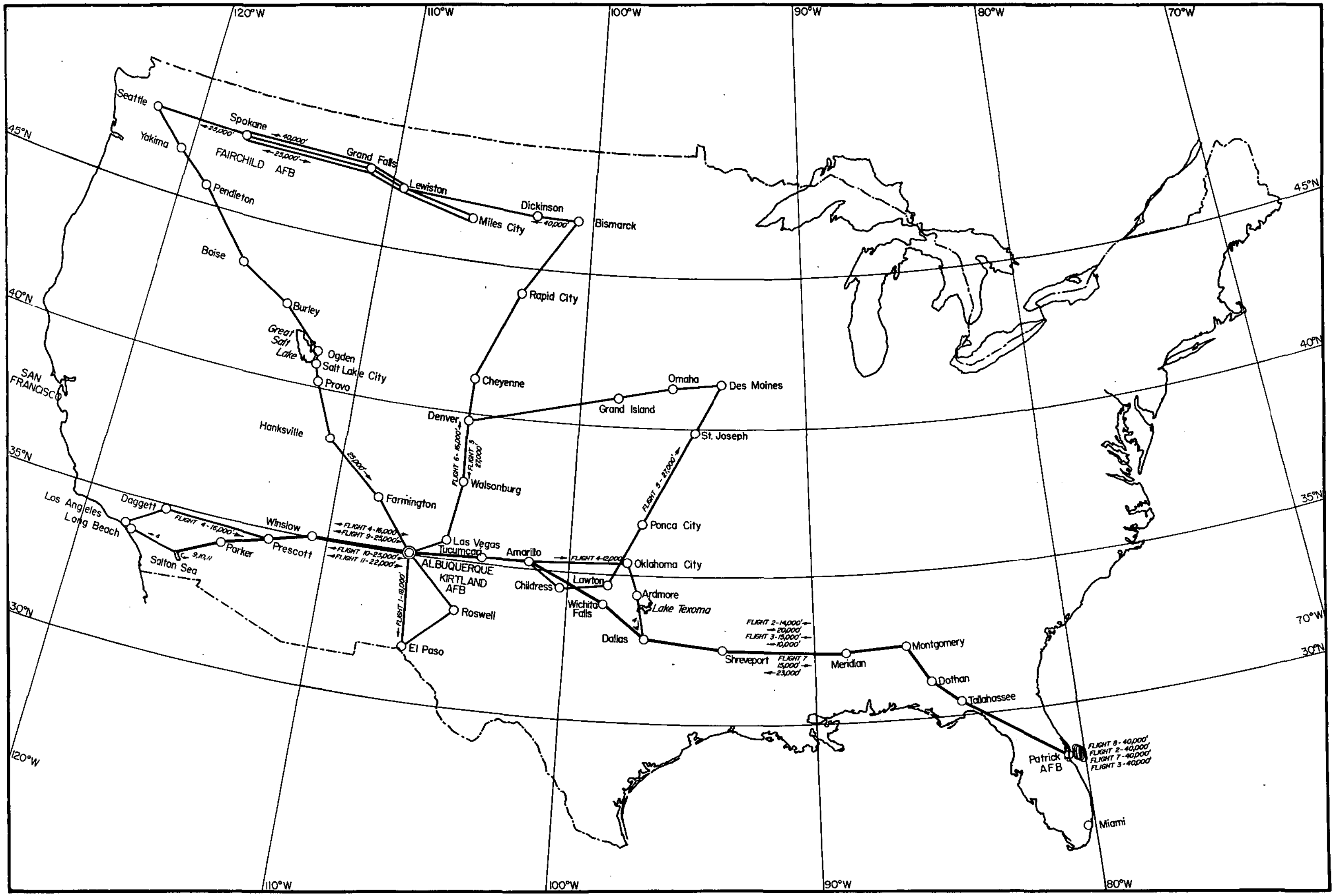

COSMIC RAY FLIGHT ROUTE

MUB-263

UCRL-8628

Fig. 2.

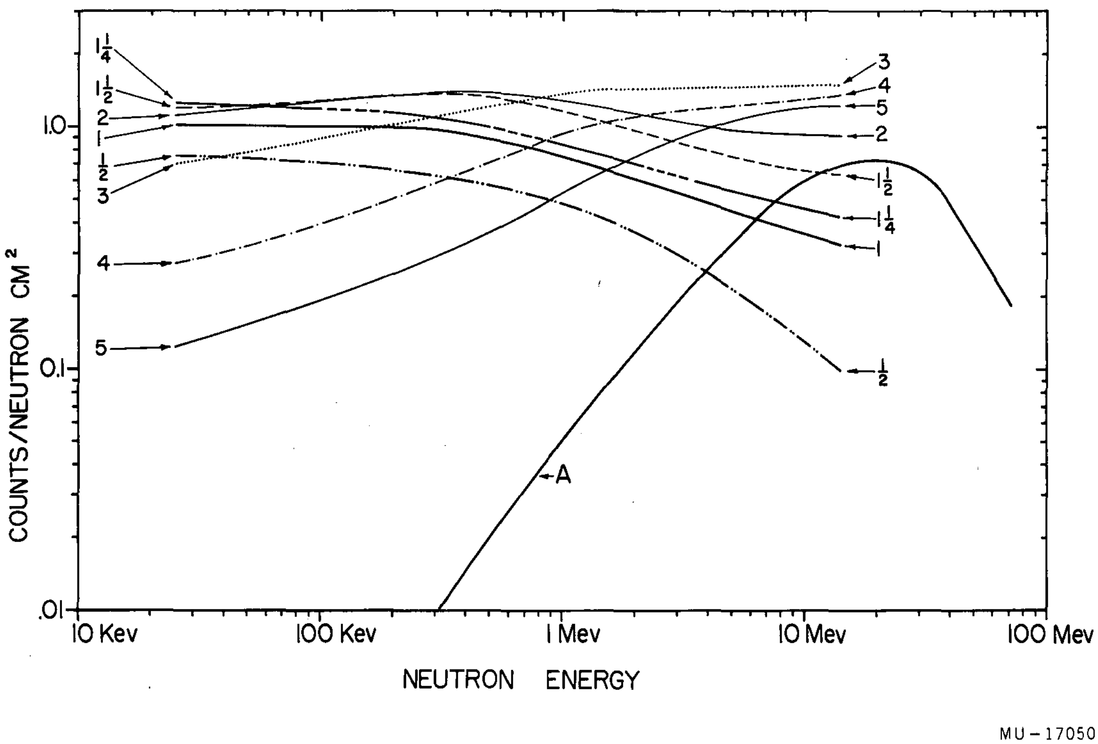
COUNTS/NEUTRON CM²
NEUTRON ENERGY
1.0
0.1
.01
10 Kev
100 Kev
1 Mev
10 Mev
100 Mev
1¼
1½
2
1
½
3
4
5
A
MU-17050

Fig. 3.

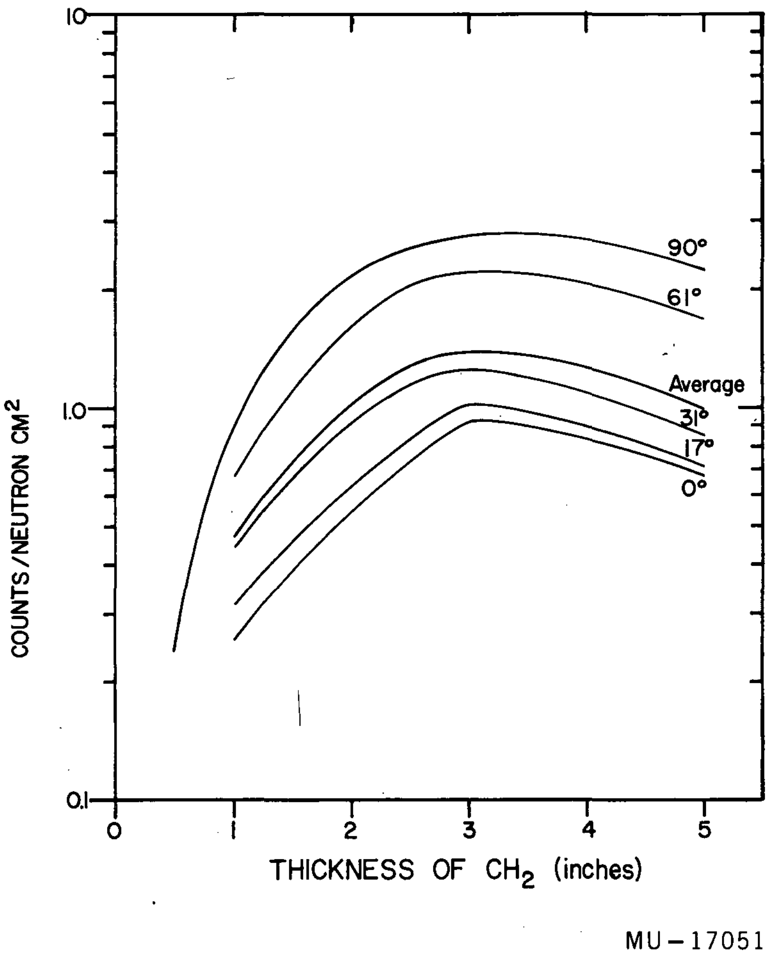
10
1.0
0.1
COUNTS/NEUTRON CM2
0
1
2
3
4
5
THICKNESS OF CH2 (inches)
90°
61°
Average
31°
17°
0°
MU-17051

Fig. 4.

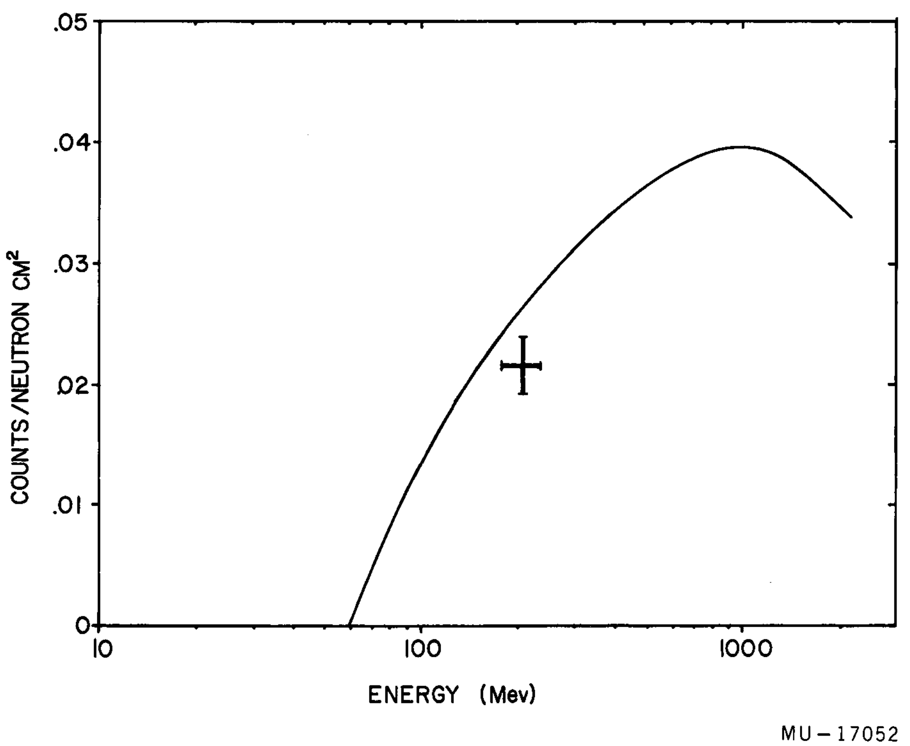
.05
.04
.03
.02
.01
0
COUNTS/NEUTRON CM2
10
100
1000
ENERGY (Mev)
MU-17052

Fig. 5.

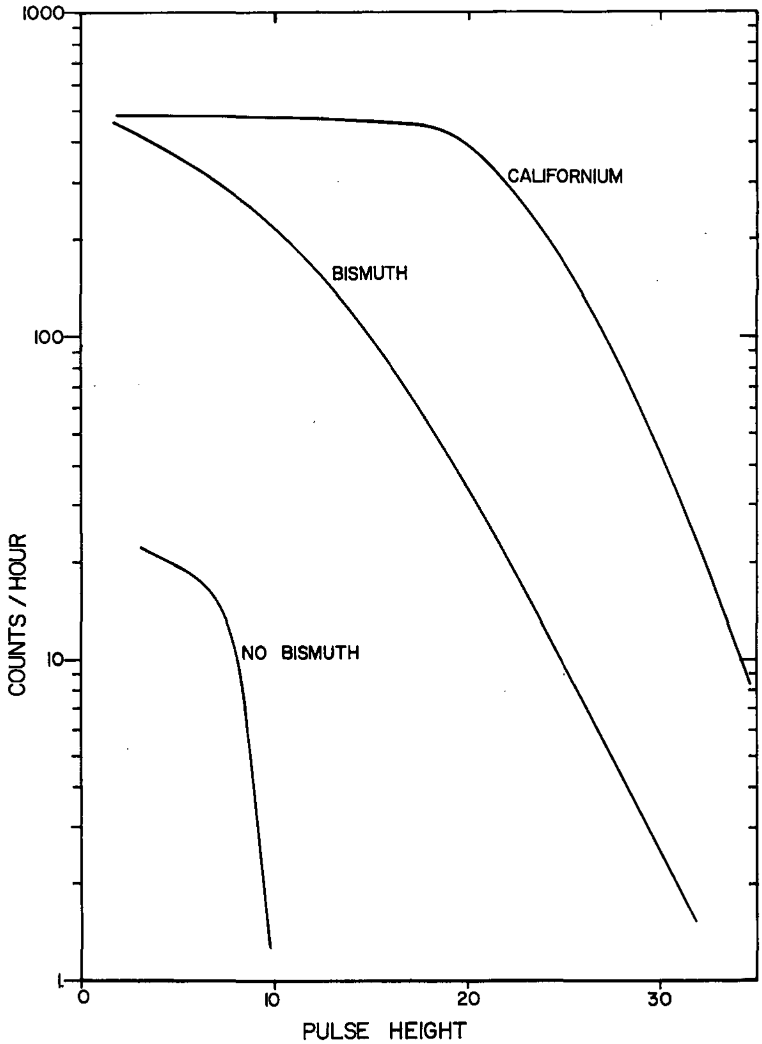

1000
100
10
1
COUNTS / HOUR
0
10
20
30
PULSE HEIGHT
CALIFORNIUM
BISMUTH
NO BISMUTH
MU-17053

Fig. 6.

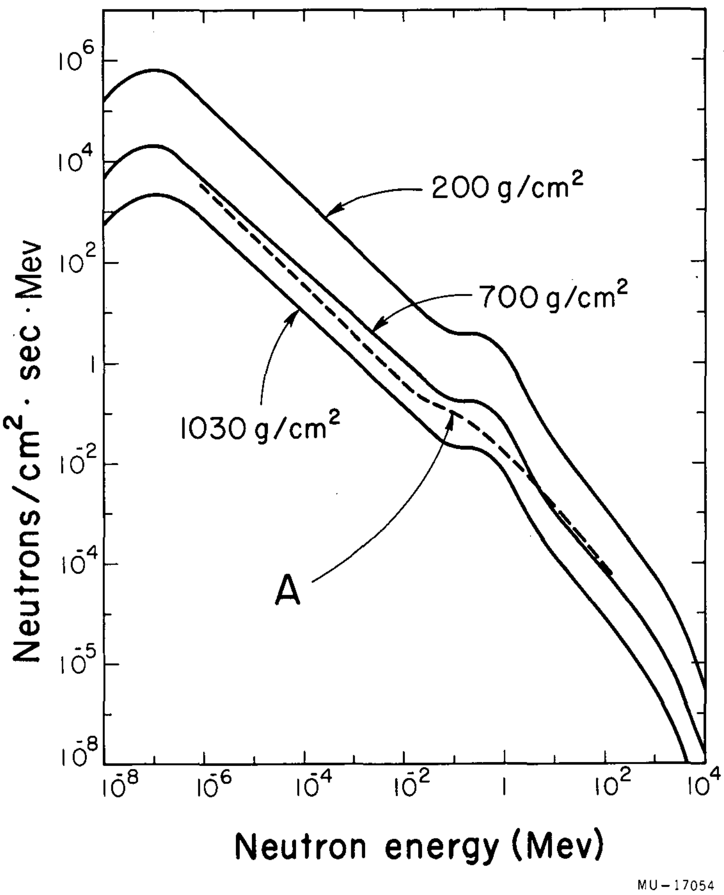

Neutrons/cm² · sec · Mev
Neutron energy (Mev)
200 g/cm²
700 g/cm²
1030 g/cm²
A
10⁶
10⁴
10²
1
10⁻²
10⁻⁴
10⁻⁵
10⁻⁸
10⁻⁸
10⁻⁶
10⁻⁴
10⁻²
1
10²
10⁴
MU-17054

Fig. 7.

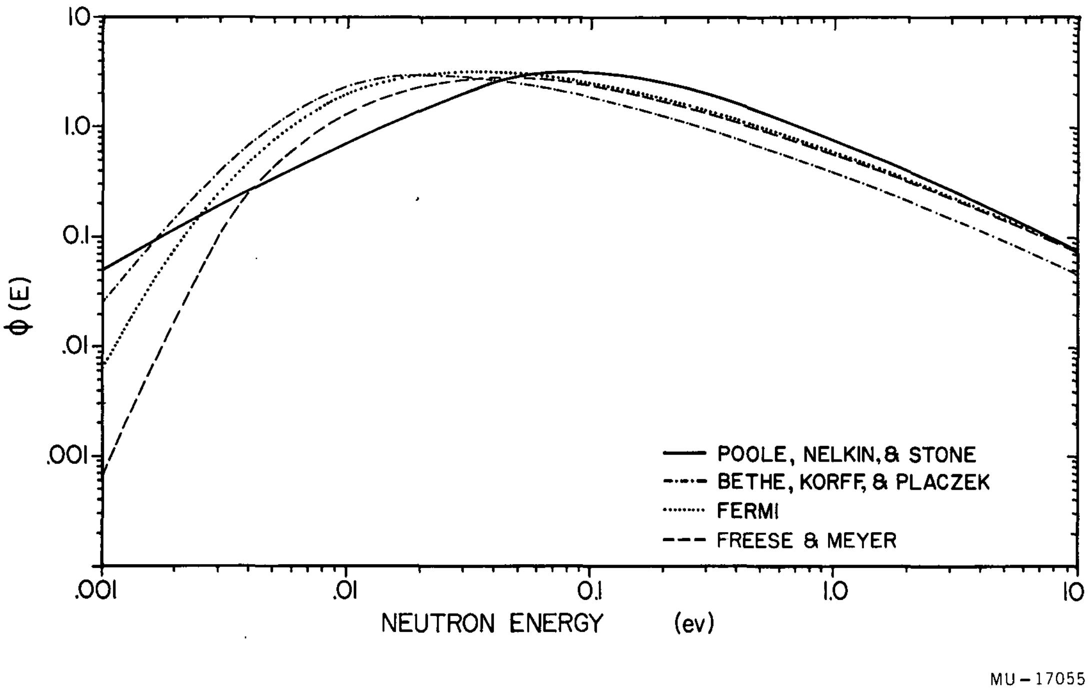
10
1.0
0.1
.01
.001
φ (E)
.001
.01
0.1
1.0
10
NEUTRON ENERGY (ev)
POOLE, NELKIN, & STONE
BETHE, KORFF, & PLACZEK
FERMI
FREESE & MEYER
MU-17055

Fig. 8.

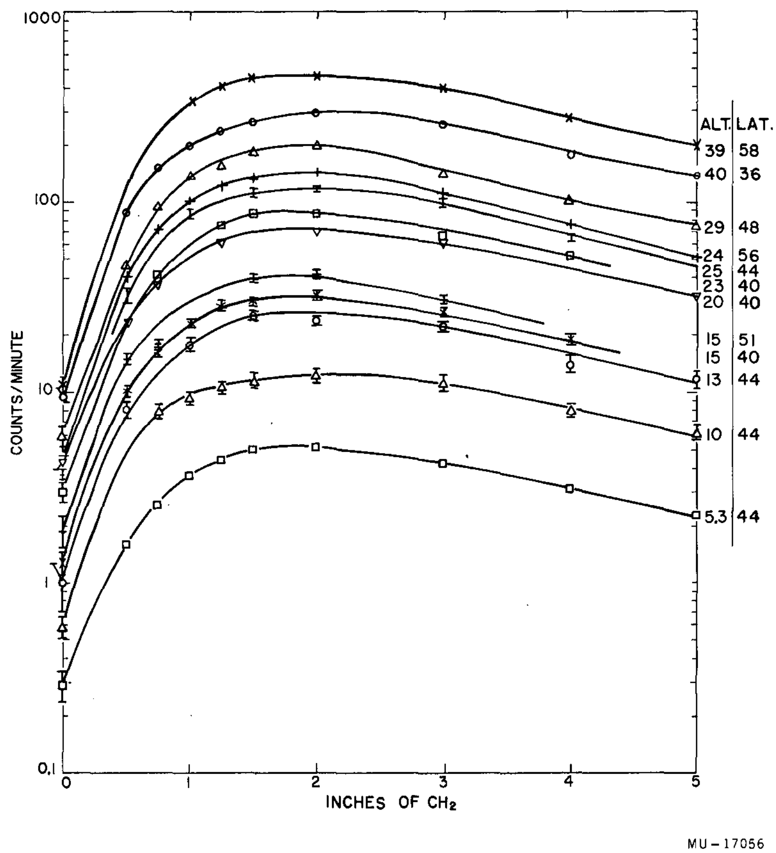
1000
100
10
1
0.1
COUNTS/MINUTE
0
1
2
3
4
5
INCHES OF CH2
ALT. LAT.
39 58
40 36
29 48
24 56
25 44
23 40
20 40
15 51
15 40
13 44
10 44
5.3 44
MU-17056

Fig. 9.

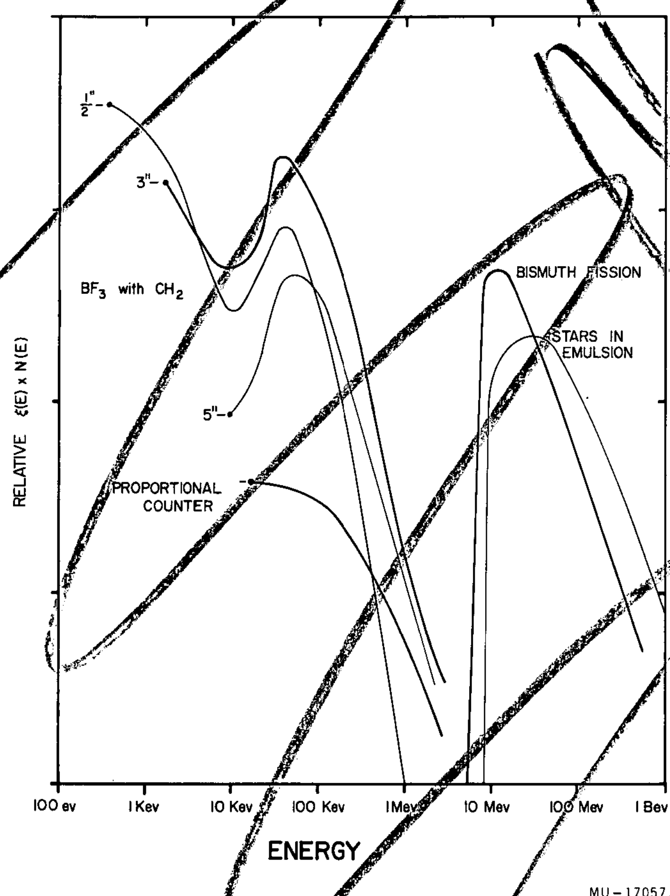
1/2"
3"
5"
BF3 with CH2
PROPORTIONAL COUNTER
BISMUTH FISSION
STARS IN EMULSION
RELATIVE ε(E) x N(E)
100 ev
1 Kev
10 Kev
100 Kev
1 Mev
10 Mev
100 Mev
1 Bev
ENERGY
MU-17057

Fig. 10.

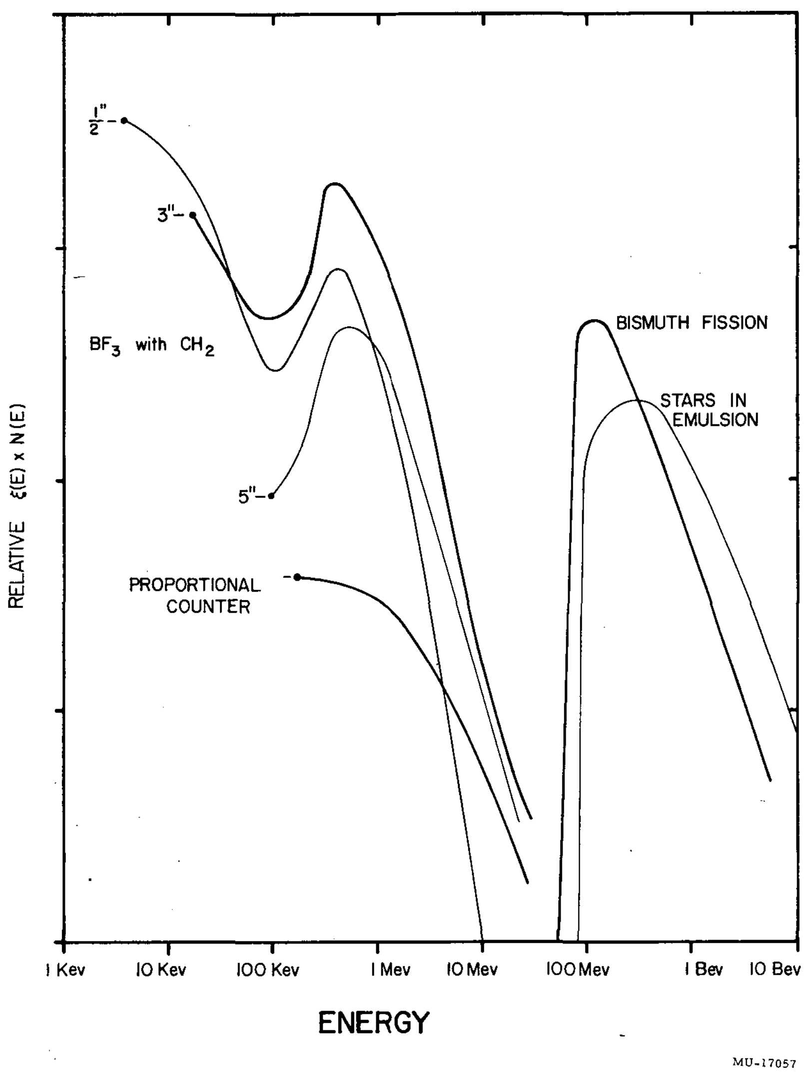

1"/2
3"
5"
BF3 with CH2
PROPORTIONAL COUNTER
BISMUTH FISSION
STARS IN EMULSION
RELATIVE ξ(E) x N(E)
1 Kev
10 Kev
100 Kev
1 Mev
10 Mev
100 Mev
1 Bev
10 Bev
ENERGY
MU-17057

Fig. 10

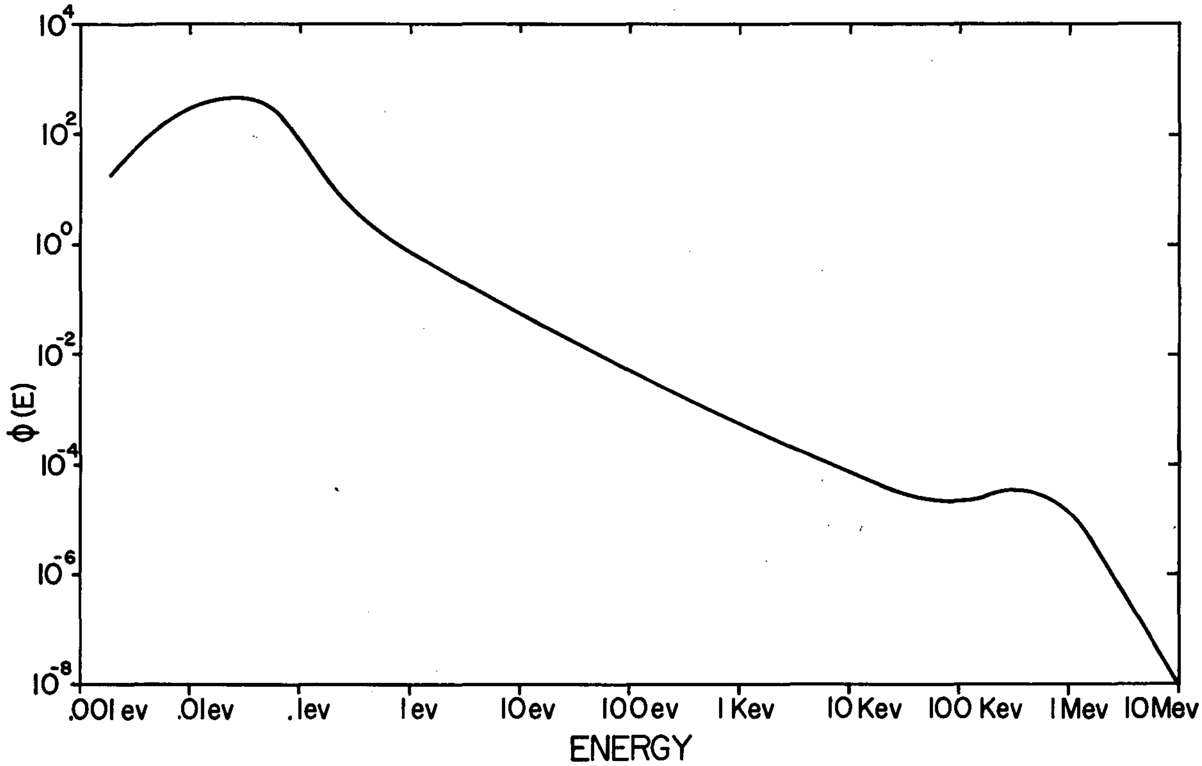

MU-17058

Fig. 11.

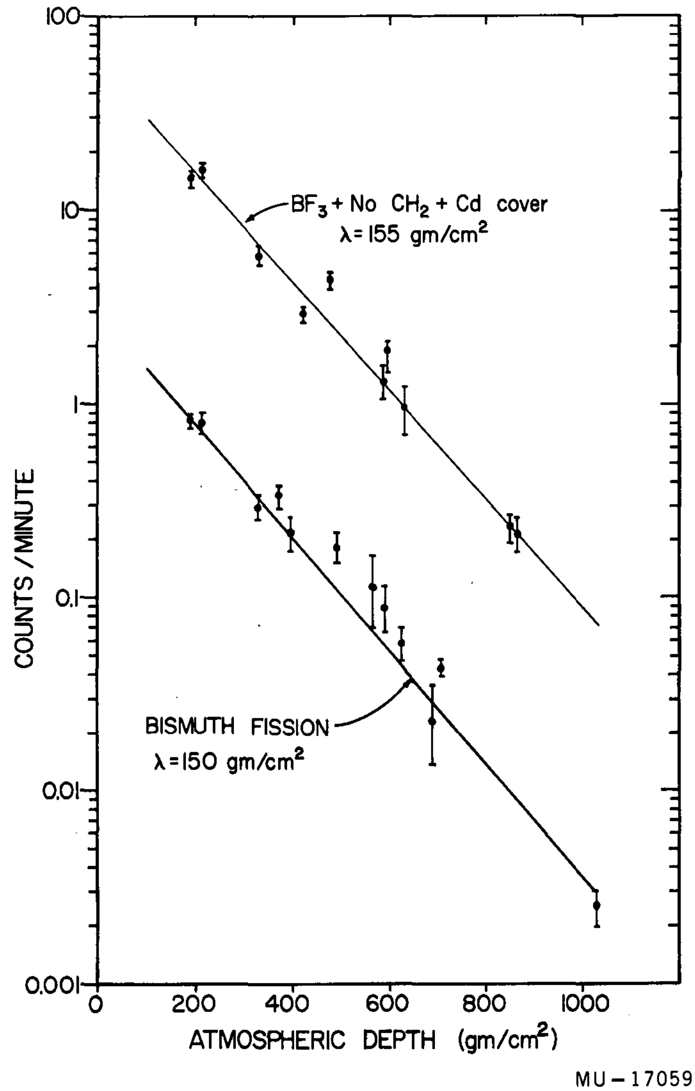
100
10
1
0.1
0.01
0.001
COUNTS / MINUTE
BF_3 + No CH_2 + Cd cover
λ = 155 gm/cm²
BISMUTH FISSION
λ = 150 gm/cm²
0
200
400
600
800
1000
ATMOSPHERIC DEPTH (gm/cm²)
MU-17059

Fig. 12.

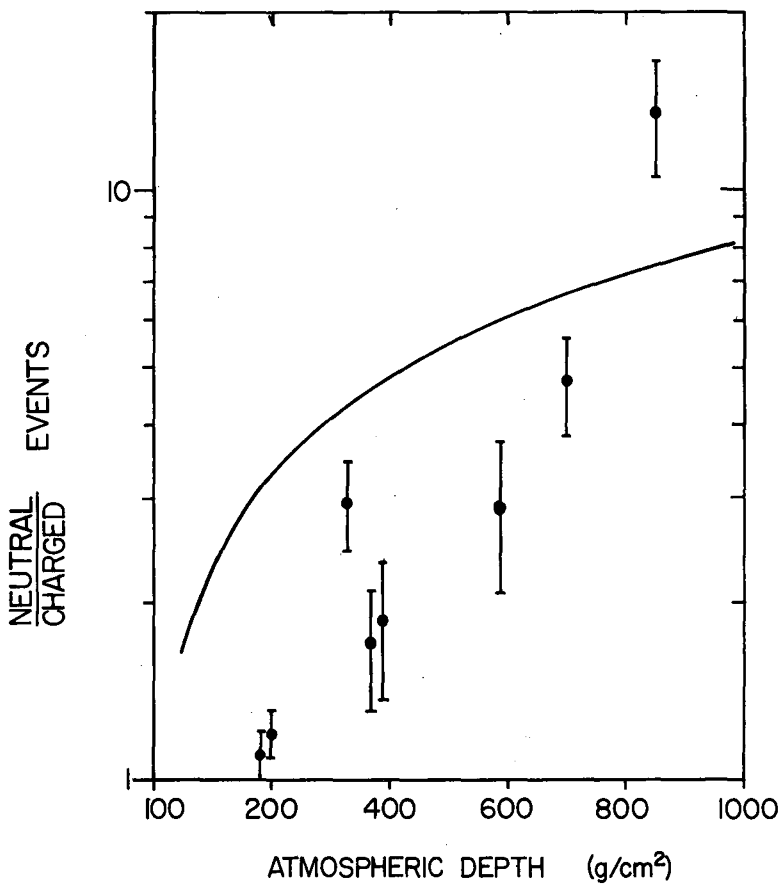

MU-17060

Fig. 13.

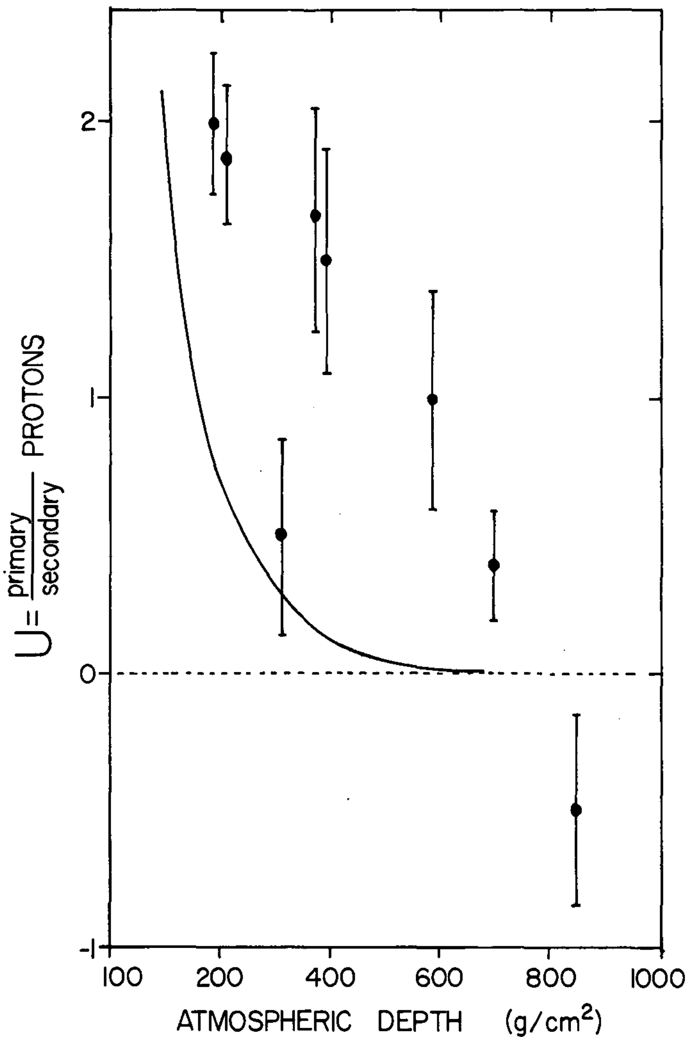

2
1
0
-1
U = primary/secondary PROTONS
100
200
400
600
800
1000
ATMOSPHERIC DEPTH (g/cm²)
MU-17061

Fig. 14.

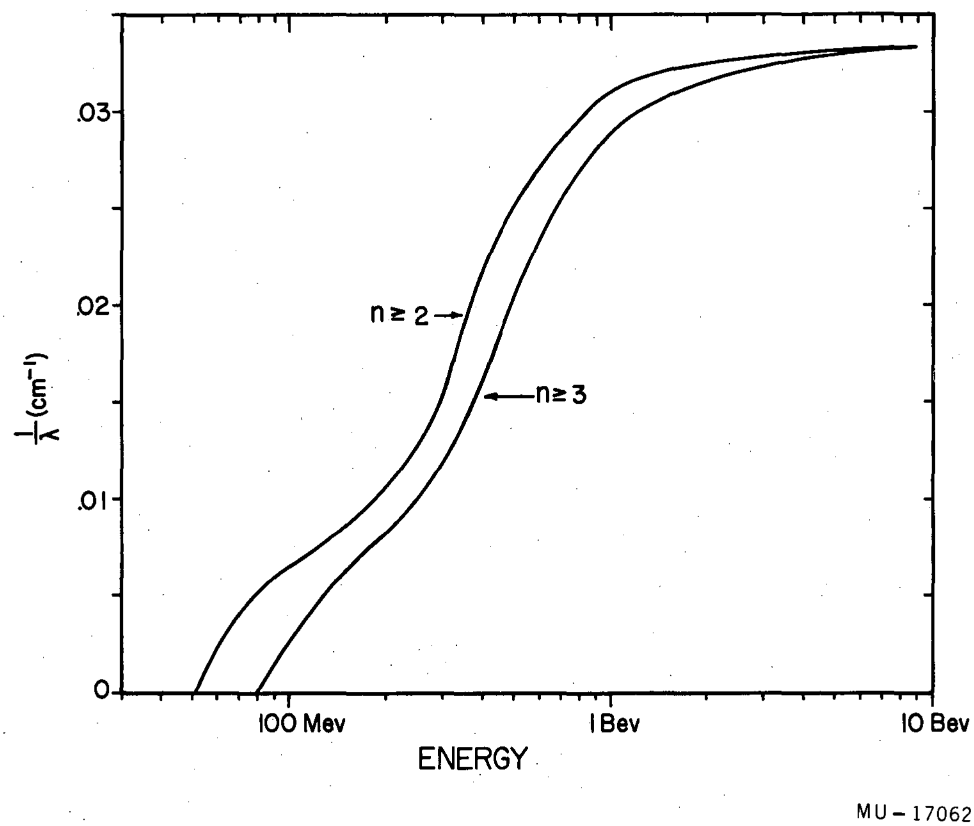
.03
.02
.01
0
$\frac{1}{\lambda}$ (cm^{-1})
n ≥ 2
n ≥ 3
100 Mev
1 Bev
10 Bev
ENERGY
MU-17062

Fig. 15.

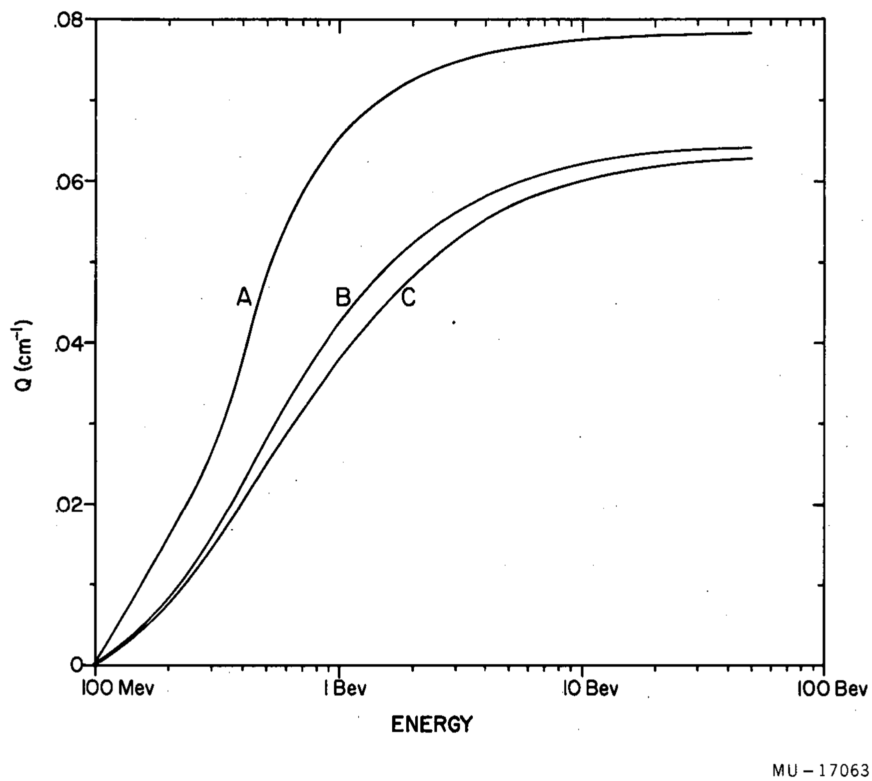
.08
.06
.04
.02
0
Q (cm^{-1})
A
B
C
100 Mev
1 Bev
10 Bev
100 Bev
ENERGY
MU – 17063

Fig. 16.